

# Juggling with light: Powerful second-order nonlinear optical effects in whispering gallery resonators!

Ingo Breunig<sup>a,b</sup> and Karsten Buse<sup>a,b</sup>

<sup>a</sup>Department of Microsystems Engineering - IMTEK, University of Freiburg,  
Georges-Köhler-Allee 102, 79110 Freiburg, Germany

<sup>b</sup>Fraunhofer Institute for Physical Measurement Techniques IPM, Heidenhofstraße 8, 79110  
Freiburg, Germany

## ABSTRACT

Whispering gallery resonators made out of crystalline materials exhibiting second-order nonlinearities enable frequency mixing such as optical parametric oscillation with high efficiency at low optical input powers and are ideally suited to realize versatile and compact optical frequency converters. Recent achievements stimulate this field further: Frequency conversion not only at a single wavelength or with few wavelengths is possible, entire frequency combs can be transferred into different spectral domains, e.g., allowing the realization of frequency combs in spectral regions that are suitable for multicomponent analytics like the mid-infrared region. Furthermore, these resonators are also supposed to be the ideal host for cascaded nonlinearities allowing the build-up of frequency combs based on second-order nonlinearities. All this comes with new and better schemes to tune whispering gallery resonators, providing advanced opportunities to modulate the laser wavelengths with nanosecond speed employing the Pockels effect. Juggling with light: We will summarize in the presentation these recent achievements, demonstrating that in the field of whispering gallery resonators still many discoveries are ahead of us.

**Keywords:** Nonlinear optics, Optical parametric oscillators, Whispering gallery modes

## 1. INTRODUCTION

Whispering gallery resonators (WGRs) guide light by total internal reflection along the rim of a spheroidally-shaped dielectric having the major and minor radii  $R$  and  $\rho$ , respectively (Fig. 1a). As sketched in Fig. 1b, the spatial electric-field distribution of a monochromatic intracavity light wave is characterized by three mode numbers  $m$  (number of oscillations in azimuthal direction),  $p$  (numbers of zeros in polar direction) and  $q$  (number of extrema in radial direction). Each electric-field distribution, i.e. the whispering gallery mode, is associated with its resonance frequency

$$\nu_{m,p,q} = \frac{mc_0}{2\pi R n_{\text{eff}}} \quad (1)$$

with the vacuum speed of light  $c_0$  and with the effective refractive index  $n_{\text{eff}}$  that depends on the shape of the resonator and on the three mode numbers. Furthermore,  $n_{\text{eff}}$  is a function of the bulk refractive index, i.e. of the resonator temperature and of the light polarization.

Since the intracavity light is guided by total internal reflection. The quality factor of the resonator can reach outstandingly high values,  $Q = 10^{11}$  has been demonstrated.<sup>1</sup> In combination with the fact that the light field is strongly localized close to the rim of the resonator, this leads to a strong intensity enhancement. Consequently, whispering gallery resonators are ideally suited for nonlinear-optical applications.<sup>2</sup> The symmetry of the resonator material dictates which nonlinear-optical effects can occur. In centrosymmetric materials, the DC Kerr effect, i.e. the quadratic electro-optic effect, changes the refractive index of the material and consequently the resonance frequency  $\nu_{m,p,q}$  in presence of an external electric field. In most materials, this effect can be neglected.<sup>3</sup> However, close to the transition between a paraelectric and a ferroelectric phase of some crystal

---

Further author information: (Send correspondence to I.B.)

I.B.: E-mail: optsys@ipm.fraunhofer.de, Telephone: +49 761 203 7455

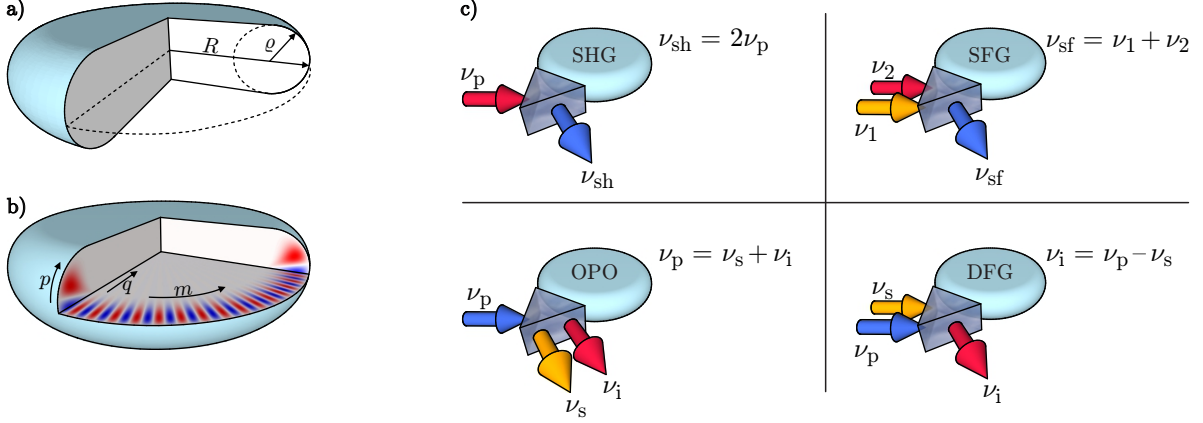


Figure 1. a) Spheroidal shape of a whispering gallery resonator with the major and minor radii  $R, \rho$ . b) The spatial electric field distribution of the circulating light is characterized by the mode numbers  $m, p, q$ . c) Basic frequency conversion processes based on the second-order optical nonlinearity in whispering gallery resonators with the respective input and output frequencies  $\nu_j$ . Second harmonic generation (SHG), sum frequency generation (SFG), optical parametric oscillation (OPO), difference frequency generation (DFG).

compounds, a considerable dc Kerr effect is observed.<sup>4,5</sup> Furthermore, centrosymmetric materials provide four-wave mixing processes which are the base of frequency-comb generation in microresonators.<sup>6</sup>

In Non-centrosymmetric materials, we find additionally second-order optical nonlinearities such as the Pockels effect, i.e. the linear electro-optic effect. Here, the refractive index  $n$  of a material changes by  $\Delta n = -n^3 r E / 2$  with the electro-optic coefficient  $r$  and the external electric field  $E$ . Substituting this into Eq. (1), we obtain

$$\Delta\nu_{m,p,q} = \frac{1}{2}\nu_{m,p,q}n_{\text{eff}}^2 r E \quad (2)$$

for the shift of the resonance frequency of a whispering gallery resonator made of a non-centrosymmetric material. For typical values  $\nu_{m,p,q} = 300$  THz,  $n_{\text{eff}} = 2$ ,  $r = 10$  pm/V and  $E = 100$  V/mm, we get a shift of 600 MHz. Besides the Pockels effect, non-centrosymmetric materials provide the basic three-wave mixing processes sketched in Fig. 1c, namely second harmonic generation (SHG), sum frequency generation (SFG), difference frequency generation (DFG) and optical parametric oscillation (OPO). In particular the latter enables the realization of millimeter-sized frequency converters tunable across hundreds of nanometers driven by a laser diode with output powers in the mW range.<sup>7</sup>

In the following, we will summarize recent advances provided by second-order nonlinearities in whispering gallery resonators made of non-centrosymmetric materials. In particular, we review basic conversion processes such as harmonic generation and optical parametric oscillation, the transfer of frequency combs into different spectral ranges as well as the generation of frequency combs by cascading different second-order nonlinearities. Furthermore, we show that adiabatic frequency conversion which does not rely on optical nonlinearities in general, can strongly benefit from the Pockels effect.

## 2. BASIC SECOND-ORDER FREQUENCY CONVERSION PROCESSES

The most investigated basic frequency conversion processes based on the second-order optical nonlinearity are frequency doubling and optical parametric oscillation. For the first, a pump wave at the frequency  $\nu_p$  is converted to its second harmonic at  $\nu_{sh} = 2\nu_p$ . In order to achieve phasematching for this process, the condition  $m_{sh} = 2m_p + M$  has to be fulfilled with the azimuthal mode numbers  $m_{p,sh}$  for the interacting waves and  $M$  reflecting a spatial variation of the second-order nonlinearity along the propagation path of the light fields. For a constant nonlinearity, we have  $M = 0$ . Under the assumption that the frequencies of both waves coincide with resonant

frequencies and phasematching is fulfilled, we have<sup>7</sup>

$$P_p^{\max} = \nu_p \frac{\pi \varepsilon_0 n_p^4 n_{\text{sh}}^2}{2d^2} \frac{1}{Q_{0p}^2 Q_{0\text{sh}}} V_{\text{eff}} \frac{(1+r_p)^3 (1+r_{\text{sh}})}{r_p} \quad (3)$$

for the pump power required to reach the maximum efficiency

$$\eta_{\text{sh}}^{\max} = \frac{r_p}{1+r_p} \frac{r_{\text{sh}}}{1+r_{\text{sh}}}, \quad (4)$$

with the refractive indices  $n_{p,\text{sh}}$ , the effective second-order nonlinear coefficient  $d$ , the intrinsic quality factors  $Q_{0p,0\text{sh}}$ , the effective mode volume  $V_{\text{eff}}$  and the coupling coefficients  $r_{p,\text{sh}}$ . For realistic values  $\nu_p = 300$  THz,  $n_{p,\text{sh}} = 2$ ,  $d = 1$  pm/V,  $Q_{0p,0\text{sh}} = 5 \times 10^7$ ,  $V_{\text{eff}} = 10^6$   $\mu\text{m}^3$ ,  $r_{p,\text{sh}} = 1$ , we find 25 % maximum conversion efficiency at 35  $\mu\text{W}$  pump power.

Experimental studies started in 2004 with the pioneering experiment by a team from the Jet Propulsion Laboratory in the United States. They presented the first frequency doubler based on a millimeter-sized whispering gallery resonator.<sup>8</sup> Already in this first demonstration, 50 % conversion efficiency was achieved at 25 mW pump power. Several further successful demonstrations of WGR-based second harmonic generation followed. These systems were operated from the ultraviolet to the near infrared.<sup>7</sup> For more than ten years, the conversion efficiencies reached by millimeter-sized systems based on resonators made of bulk crystals have been orders of magnitude higher than the ones reached by chip-integrated resonators. This was due to the fact that the latter did not reach high quality factors. However, improved fabrication techniques have considerably changed this situation. Chip-integrated resonators with 50  $\mu\text{m}$  diameter made of aluminum nitride have been applied to obtain more than 15 % conversion efficiency at 115  $\mu\text{W}$  pump power.<sup>9</sup> This paves the way for the realization of efficient chip-integrated and robust frequency doublers.

In a whispering-gallery-based optical parametric oscillator, pump light at the frequency  $\nu_p$  is converted to signal and idler light at  $\nu_{s,i}$  such that  $\nu_p = \nu_s + \nu_i$ . Here, the phasematching condition reads  $m_p = m_s + m_i + M$ . Under the assumption that all interacting waves are perfectly at resonance and phasematching is fulfilled, the process starts at the pump threshold<sup>7</sup>

$$P_p^{\text{th}} = \nu_p \frac{\pi \varepsilon_0 n_p^2 n_s^2 n_i^2}{16d^2} \frac{1}{Q_{0p} Q_{0s} Q_{0i}} V_{\text{eff}} \frac{(1+r_p)^2 (1+r_s)(1+r_i)}{r_p} \quad (5)$$

and reaches the maximum conversion efficiency

$$\eta_{s,i}^{\max} = \frac{\nu_{s,i}}{\nu_p} \frac{r_p}{1+r_p} \frac{r_{s,i}}{1+r_{s,i}} \quad (6)$$

at  $P_p^{\max} = 4P_p^{\text{th}}$ . Comparing these expressions with the above-mentioned ones for second harmonic generation, one can see that WGR-based OPOs can reach conversion efficiencies of several 10 percent at pump powers below 1 mW.

First indications of highly nondegenerate optical parametric oscillation generating idler light with frequencies of several hundred Gigahertz in a whispering gallery resonator have been published in 2007.<sup>10</sup> However, the idler light could not be detected directly. The first experimental proof of optical parametric oscillation in a WGR was published three years later.<sup>11</sup> Various demonstrations on WGR-based optical parametric oscillators followed.<sup>7</sup> Hundreds on nanometers tunability of the output wavelengths by changing the resonator temperature or the radial mode number of the pump wave have been shown (Fig. 2a). Most devices were based so far on lithium niobate. They covered wavelengths from below 0.6 to 3  $\mu\text{m}$  wavelength (Fig. 2b). The tuning range of WGR-based OPOs was extended into the mid infrared even by applying resonators made of CdSiP<sub>2</sub><sup>12</sup> and AgGaSe<sub>2</sub>.<sup>13</sup> Typically, WGR-based OPOs are operated at pump powers from several  $\mu\text{W}$  to ten mW.<sup>11,12</sup> Efficiencies of several ten percent are readily achievable.<sup>14</sup> Furthermore, stable single-frequency operation as well as mode-hop-free tuning of the output wavelengths is possible.<sup>14,15</sup> Recently, the first chip-integrated ring-resonator-based optical parametric oscillator was demonstrated using aluminum nitride.<sup>16</sup>

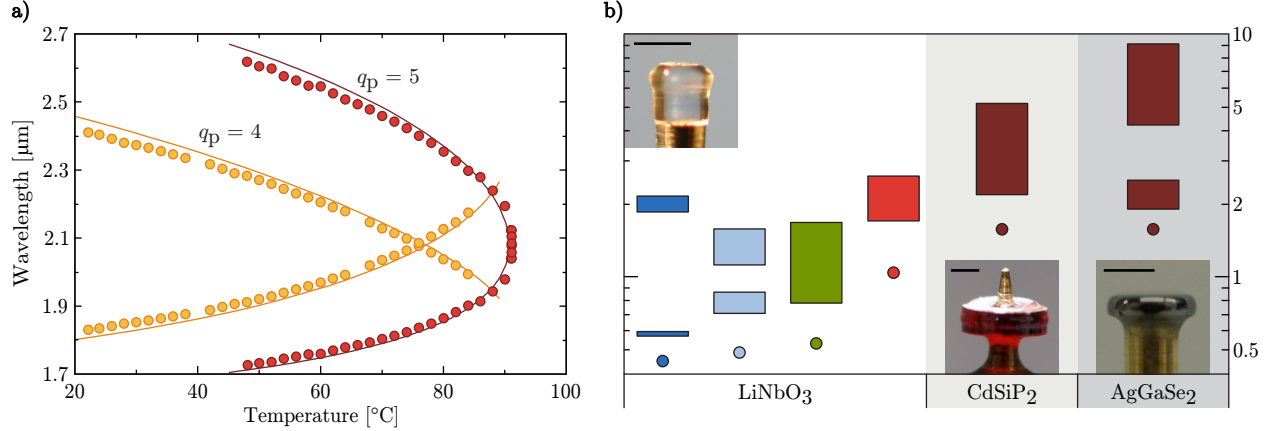


Figure 2. a) Wavelength tuning of a whispering gallery optical parametric oscillator by changing the resonator temperature for two different radial mode numbers  $q_p$  of the pump light.<sup>17</sup> b) Spectral coverage of WGR-based OPOs made of different materials for different pump wavelengths indicated by the circles (450, 488, 532, 1040, 1570 nm).<sup>7,12,13</sup> The photographs show WGRs made of the respective materials. The scale bar measures 1 mm.

### 3. FREQUENCY-COMB TRANSFER AND GENERATION

Applying optical microresonators has revolutionized the generation of frequency combs. Nowadays, chip-integrated devices exist based on various material platforms.<sup>6</sup> They can even be battery powered.<sup>18</sup> They are applied for spectroscopy, telecommunications, pulse shaping, frequency synthesis, distance ranging, astronomy, and biological imaging.<sup>6</sup> The vast majority of frequency combs is operated in the telecom spectral range, i.e. around 1.5 μm wavelength. However, many applications such as astronomical spectroscopy, quantum physics, optical clocks, and molecular sensing require the frequency comb to be centered in the visible (VIS), ultra-violet (UV), or mid-infrared (MIR).

The above-mentioned basic second-order nonlinear frequency conversion processes can be used to transfer a frequency comb into other spectral ranges. Second harmonic generation and sum frequency generation will shift the comb to higher frequencies and optical parametric oscillation to lower ones (see Fig. 3a). We have demonstrated this with a high-repetition-rate (10.5 GHz) near-infrared frequency comb centered around 1565 nm wavelength.<sup>19</sup> Here, a millimeter-sized whispering gallery resonator made of lithium niobate with 21 GHz free spectral range serves as frequency converter, i.e. we used subharmonic synchronous pumping. Second-harmonic generation transfers the comb into the red spectral range (centered around 783 nm wavelength). Simultaneously, sum frequency mixing of the pump light with its second harmonic generates a comb around the third harmonic centered around 522 nm wavelength. Furthermore, the comb in the red spectral range is frequency doubled. This leads to the generation of a frequency comb in the ultraviolet spectral range (centered around 391 nm wavelength). Thus, we end up with four frequency combs from the NIR to the UV (Fig. 3b). In order to achieve phasematching for all processes simultaneously, a quasi-phasematching structure providing  $M = 283$  for second harmonic generation,  $M = 1746$  for third harmonic generation as well as  $M = 2618$  for fourth harmonic generation is needed. This is achieved by imprinting a chirped pattern of ferroelectric domains via calligraphic poling into the resonator material.<sup>20</sup>

The transfer of the frequency comb into the mid infrared was demonstrated as well. Here, the millimeter-sized resonator made of lithium niobate had a quasi-phasematching structure formed by parallel ferroelectric domains with 30.5 μm periodicity. The near infrared frequency comb centered around 1559 nm wavelength was transferred to its subharmonic via optical parametric oscillation, i.e. to 3118 nm wavelength. Here, degenerate and non-degenerate operation was achieved. The experimental setup can be considerably simpler when the generation of a frequency comb and the transfer take place in the same cavity. One approach is to generate a Kerr comb via third-order nonlinearity in a resonator made of a non-centrosymmetric material and to use the intrinsic second-order nonlinearity to convert the Kerr comb into another spectral range. This was demonstrated in resonators made of aluminum nitride,<sup>22</sup> gallium phosphide<sup>23</sup> and lithium niobate.<sup>24</sup>

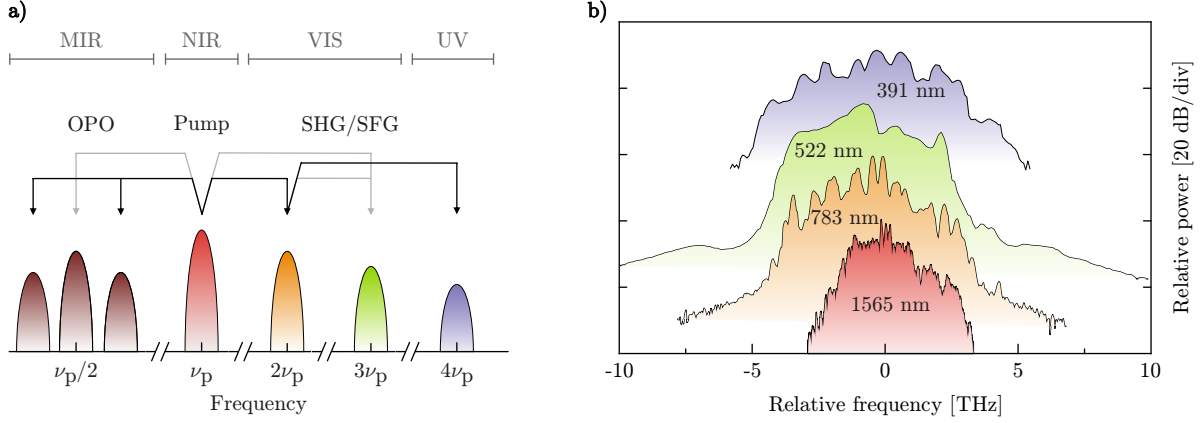


Figure 3. a) Scheme for transferring a near infrared frequency (NIR) comb centered around the pump frequency  $\nu_p$  into the infrared (MIR), visible (VIS) and ultraviolet (UV) spectral ranges by second-order optical nonlinearities. b) Spectra of the initial frequency comb at 1565 nm wavelength and of the transferred combs at the second, third and fourth harmonic.<sup>19</sup>

There is, however, a more elegant way to generate frequency combs at both the pump frequency and its second-harmonic simultaneously. It is based on second-order nonlinearities only and relies on cascaded second-order nonlinear-optical processes<sup>25</sup> (see Fig. 4a). This process might be driven at much lower pump thresholds since for continuous-wave light the second-order nonlinearity is generally much stronger than the third-order one. Although the idea has been around for almost two decades, so far only few experimental realizations are known, based either on bulky bow-tie cavities<sup>26,27</sup> or on relatively low- $Q$  waveguide resonators.<sup>28</sup> Recently, we have presented this scheme in a high- $Q$  millimeter-sized whispering gallery made of lithium niobate.<sup>21</sup> Here, we pump the resonator at 1064 nm wavelength generating first its second harmonic in the green spectral region. At 2 mW pump power, we observe two 2 THz wide frequency combs, one around the pump wavelength and one around 532 nm wavelength (see Fig. 4b). The separation between the comb lines is 21 GHz. This is close to the free spectral range at the pump wavelength and significantly larger than the one around the second-harmonic (19.5 GHz), i.e. the pump wave seems to dictate the free spectral range of both frequency combs.

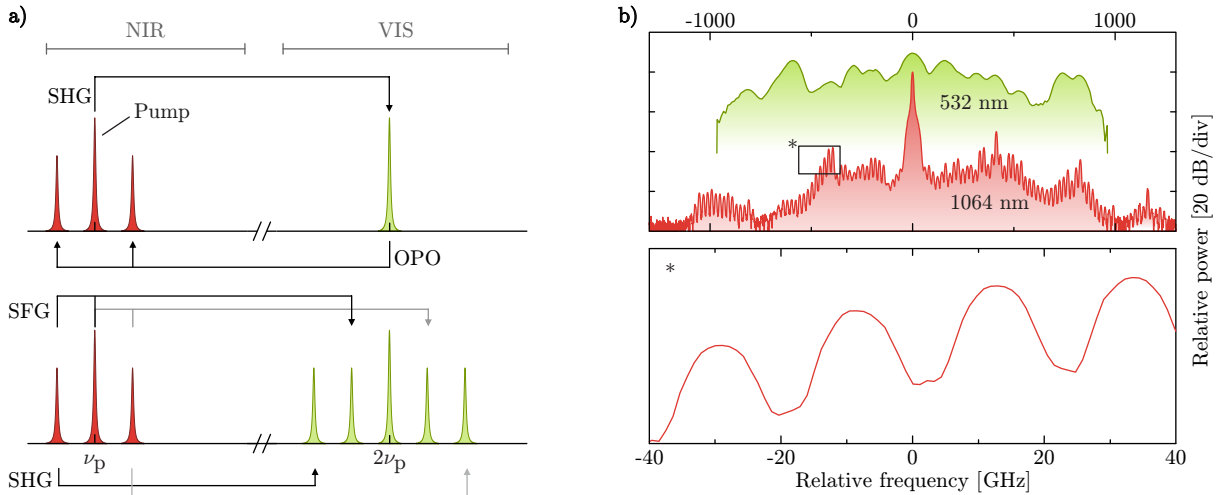


Figure 4. a) Scheme for the generation of two frequency combs using second-order optical nonlinearities. b) output spectra of the two frequency combs centered around the pump wavelength at 1064 nm and around its second harmonic at 532 nm. The zoom shows individual spectral components separated by 21 GHz.<sup>21</sup>

## 4. ADIABATIC FREQUENCY CONVERSION

Optical frequency conversion based on nonlinear optics in microresonators as described above has been advanced over the last decades. It is based on the nonlinear response of the material to laser light. High conversion efficiencies require high light intensities. Furthermore, the phases of the interacting waves have to be matched. An alternative optical frequency conversion technique is adiabatic frequency conversion (AFC). Here, the frequency of light traveling in a resonator is shifted due to a change of the optical length of a round-trip, i.e. one can change the refractive index of the material and keep the geometrical path length constant. The frequency of light changes then according to<sup>29</sup>

$$\frac{\Delta\nu}{\nu_p} = -\frac{\Delta n}{n_p}. \quad (7)$$

Thus, the intracavity light strictly follows the shift of the resonance frequency. In order to achieve AFC, the refractive index has to be changed faster than the decay time of the cavity. This is the only requirement. In contrast to nonlinear-optical frequency conversion, no intense laser light is necessary, nor additional effort has to be taken for phasematching. In previous studies on adiabatic frequency conversion in microresonators the refractive index was changed via injecting charges by means of ultra-short laser pulses<sup>30</sup> or by means of electric pumping<sup>31</sup> or via the AC Kerr effect.<sup>32</sup> Charge injection provides positive frequency shifts in the 100-GHz range. However, the quality factor is fairly low ( $2 \times 10^4$ ) due to the generation of free charges. In contrast to this, employing the AC Kerr effect enables just negative frequency changes limited to the 100-MHz range, but a high quality factor of the cavity can be maintained ( $> 10^7$ ). None of the schemes demonstrated so far combined a wide tuning range with the flexibility to chose the sign of the shift and with preserving a high quality factor.

We have demonstrated recently adiabatic frequency conversion driven by the Pockels effect, i.e. the linear electro-optic effect.<sup>33</sup> Evaluating Eq. (2) for the shift of the resonance frequency due to the Pockels effect, we see that the shift is strictly linear with respect to the external electric field. Thus, by changing its sign, we can change between blue and red frequency shifts. Furthermore, the Pockels effect does not influence the quality factor. In our proof-of-concept experiment, we have fabricated a millimeter-sized and 70- $\mu\text{m}$ -thick whispering gallery resonator made of lithium niobate. The electric field is applied between electrodes on the top and bottom faces of the WGR (see Fig. 5a). First, we tune the pump frequency  $\nu_p$  to a whispering gallery resonance and load the cavity via a coupling prism. When the cavity is loaded, we switch on the voltage. Then, the pump light is totally reflected at the prism base and the frequency of the intracavity light is shifted to  $\nu_{\text{out}}$ . At the output facet of the prism, we detect a beat signal with  $\Delta\nu = \nu_{\text{out}} - \nu_p$  (see Fig. 5b). It reflects the frequency shift. As expected, the shift is directly proportional to the applied voltage (see Fig. 5c). At only 20 V, we achieve 5 GHz tuning. This is already more than one order of magnitude larger than the frequency shift obtained applying the AC Kerr

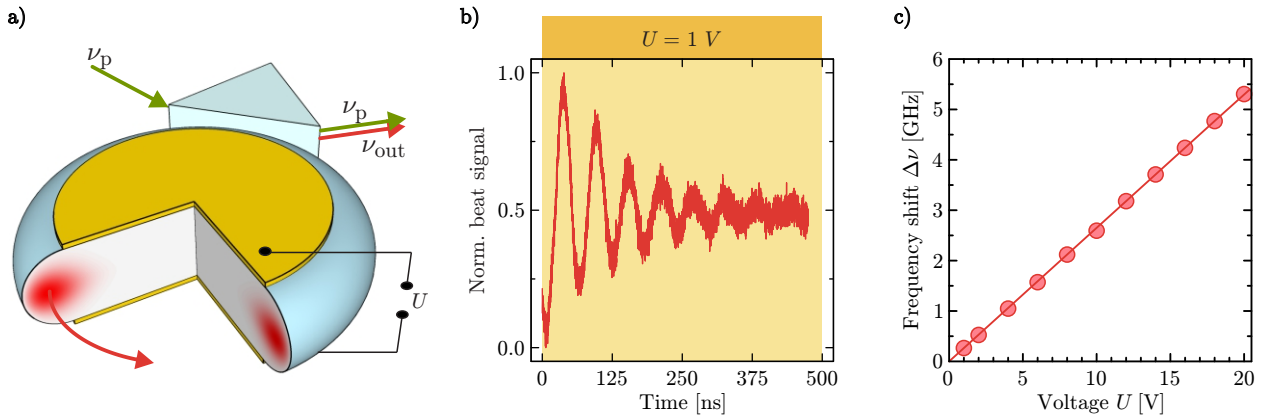


Figure 5. a) Sketch of the experimental setup for adiabatic frequency conversion comprising the whispering gallery resonator with electrodes and the coupling prism. The frequency  $\nu_p$  of the pump light is converted to  $\nu_{\text{out}}$  by applying the voltage  $U$ . b) Beat signal between the pump light at  $\nu_p$  and the converted light at  $\nu_{\text{out}}$ . c) Linear dependence between frequency shift  $\Delta\nu = \nu_{\text{out}} - \nu_p$  and voltage  $U$ .<sup>33</sup>

effect. Here, we are limited only by the maximum voltage of the function generator used. It was demonstrated that electric fields as large as 65 kV/mm can be applied to lithium niobate crystals without damaging them.<sup>34</sup> Such electric fields would induce refractive-index changes of  $10^{-3}$  and consequently frequency shifts in the THz range.

## 5. CONCLUSION

The above-mentioned results highlight the huge potential of second-order nonlinearities in microresonator-based frequency converters. Already now, we see highly efficient compact and wavelength flexible devices. They are operated from the UV to the MIR. In particular, the recent advances in chip-integration will further boost this development. We are not far away anymore from the realization of miniaturized frequency converters that will successfully operate in out-of-the-lab applications. After the successful demonstration of frequency combs via second-order nonlinearities in a microresonator, new scientific discoveries are ahead of us. In contrast to Kerr combs, we deal with two or more subcombs in spectral regions with considerably different group velocities. Frequency-comb generation including non-degenerate optical parametric oscillation is almost unexplored. Employing the Pockels effect for adiabatic frequency conversion has also the potential to drive this scheme out of the lab. The setup is considerably simpler compared with the previous implementations. It combines large tunability with high quality factors and an unprecedented flexibility regarding the frequency shift. In principle, arbitrary waveforms like linear or nonlinear chirps can be generated easily. We conclude that after 15 years of nonlinear optics in whispering gallery resonators, fascinating discoveries and developments are still ahead of us.

## REFERENCES

- [1] Savchenkov, A. A., Matsko, A. B., Ilchenko, V. S., and Maleki, L., “Optical resonators with ten million finesse,” *Opt. Express* **15**, 6768–6773 (2007).
- [2] Strekalov, D. V., Marquardt, C., Matsko, A. B., Schwefel, H. G. L., and Leuchs, G., “Nonlinear and quantum optics with whispering gallery resonators,” *J. Opt.* **18**, 123002 (2016).
- [3] Weber, M. J., [*Handbook of optical materials*], CRC Press, Boca Ranton (2003).
- [4] Fujiura, K. and Nakamura, K., “Ktn optical waveguide devices with an extremely large electro-optic effect,” in [*Passive Components and Fiber-based Devices*], Sun, Y., Jian, S., Lee, S. B., and Okamoto, K., eds., *Proc. SPIE* **5623**, 518 (2005).
- [5] Szabados, J., Manjeshwar, S. K., Breunig, I., and Buse, K., “Electro-optic tuning of potassium tantalate-niobate whispering gallery resonators,” in [*Laser Resonators, Microresonators, and Beam Control XX*], Kudryashov, A. V., Paxton, A. H., and Ilchenko, V. S., eds., *Proc. SPIE* **10518**, 1051802 (2018).
- [6] Gaeta, A. L., Lipson, M., and Kippenberg, T. J., “Photonic-chip-based frequency combs,” *Nat. Photon.* **13**, 1158 (2019).
- [7] Breunig, I., “Three-wave mixing in whispering gallery resonators,” *Laser Photon. Rev.* **10**, 569–587 (2016).
- [8] Ilchenko, V. S., Savchenkov, A. A., Matsko, A. B., and Maleki, L., “Nonlinear optics and crystalline whispering gallery mode cavities,” *Phys. Rev. Lett.* **92**, 043903 (2004).
- [9] Lu, J., Surya, J. B., Liu, X., Bruch, A. W., Gong, Z., Xu, Y., and Tang, H. X., “Periodically poled thin-film lithium niobate microring resonators with a second-harmonic generation efficiency of 250,000%/w,” *Optica* **6**, 1455–1460 (2019).
- [10] Savchenkov, A. A., Matsko, A. B., Mohageg, M., Strekalov, D. V., and Maleki, L., “Parametric oscillations in a whispering gallery resonator,” *Opt. Lett.* **32**, 157–159 (2007).
- [11] Fürst, J. U., Strekalov, D. V., Elser, D., Aiello, A., Andersen, U. L., Marquardt, C., and Leuchs, G., “Low-threshold optical parametric oscillations in a whispering gallery mode resonator,” *Phys. Rev. Lett.* **105**, 263904 (2010).
- [12] Jia, Y., Hanka, K., Zawilski, K. T., Schunemann, P. G., Buse, K., and Breunig, I., “Continuous-wave whispering-gallery optical parametric oscillator based on CdSiP<sub>2</sub>,” *Opt. Express* **26**, 10833–10841 (2018).
- [13] Meisenheimer, S.-K., Fürst, J. U., Buse, K., and Breunig, I., “Continuous-wave optical parametric oscillation tunable up to an 8  $\mu$ m wavelength,” *Optica* **4**, 189–192 (2017).

- [14] Werner, C. S., Buse, K., and Breunig, I., “Continuous-wave whispering-gallery optical parametric oscillator for high-resolution spectroscopy,” *Opt. Lett.* **40**, 772–775 (2015).
- [15] Werner, C. S., Yoshiki, W., Herr, S. J., Breunig, I., and Buse, K., “Geometric tuning: spectroscopy using whispering gallery resonator frequency-synthesizers,” *Optica* **4**, 1205–1208 (2017).
- [16] Bruch, A. W., Liu, X., Surya, J. B., Zou, C.-L., and Tang, H. X., “On-chip  $\chi^{(2)}$  microring optical parametric oscillator,” *Optica* **6**, 1361–1366 (2019).
- [17] Meisenheimer, S.-K., Fürst, J. U., Schiller, A., Holderied, F., Buse, K., and Breunig, I., “Pseudo-type-ii tuning behavior and mode identification in whispering gallery optical parametric oscillators,” *Opt. Express* **24**, 15137–15142 (2016).
- [18] Stern, B., Ji, X., Okawachi, Y., Gaeta, A. L., and Lipson, M., “Battery-operated integrated frequency comb generator,” *Nature* **562**, 401–405 (2018).
- [19] Herr, S. J., Brasch, V., Szabados, J., Obrzud, E., Jia, Y., Lecomte, S., Buse, K., Breunig, I., and Herr, T., “Frequency comb up- and down-conversion in synchronously driven  $\chi^{(2)}$  optical microresonators,” *Opt. Lett.* **43**, 5745–5748 (2018).
- [20] Mohageg, M., Strekalov, D. V., Savchenkov, A. A., Matsko, A., Ilchenko, V. S., and Maleki, L., “Calligraphic poling of lithium niobate,” *Opt. Express* **13**, 3408 (2005).
- [21] Szabados, J., Puzyrev, D. N., Minet, Y., Reis, L., Buse, K., Villois, A., Skryabin, D. V., and Breunig, I., “Frequency comb generation via cascaded second-order nonlinearities in microresonators,” *arXiv*, 1912.00945v2 (2019).
- [22] Guo, X., Zou, C.-L., Jung, H., Gong, Z., Bruch, A., Jiang, L., and Tang, H. X., “Efficient generation of a near-visible frequency comb via cherenkov-like radiation from a kerr microcomb,” *Phys. Rev. Applied* **10**, 014012 (2018).
- [23] Wilson, D. J., Schneider, K., Hnl, S., Anderson, M., Baumgartner, Y., Czornomaz, L., Kippenberg, T. J., and Seidler, P., “Integrated gallium phosphide nonlinear photonics,” *Nat. Photon.* **14**, 57–63 (2019).
- [24] He, Y., Yang, Q.-F., Ling, J., Luo, R., Liang, H., Li, M., Shen, B., Wang, H., Vahala, K., and Lin, Q., “Self-starting bi-chromatic LiNbO<sub>3</sub> soliton microcomb,” *Optica* **6**, 1138–1144 (2019).
- [25] Buryak, A. V., Trapani, P. D., Skryabin, D. V., and Trillo, S., “Optical solitons due to quadratic nonlinearities: from basic physics to futuristic applications,” *Phys. Rep.* **370**, 63–235 (2002).
- [26] Ulvila, V., Phillips, C. R., Halonen, L., and Vainio, M., “Frequency comb generation by a continuous-wave pumped optical parametric oscillator based cascading quadratic nonlinearities,” *Opt. Lett.* **38**, 4281–4284 (2013).
- [27] Mosca, S., Ricciardi, I., Parisi, M., Maddaloni, P., Santamaria, L., De Natale, P., and De Rosa, M., “Direct generation of optical frequency combs in  $\chi^{(2)}$  nonlinear cavities,” *Nanophotonics* **5**, 4281–4284 (2016).
- [28] Ikuta, R., Asano, M., Tani, R., Yamamoto, T., and Imoto, N., “Frequency comb generation in a quadratic nonlinear waveguide resonator,” *Opt. Express* **26**, 15551–15558 (2016).
- [29] Notomi, M. and Mitsugi, S., “Wavelength conversion via dynamic refractive index tuning of a cavity,” *Phys. Rev. A* **73**, 051803(R) (2006).
- [30] Preble, S. F., Xu, Q., and Lipson, M., “Changing the colour of light in a silicon resonator,” *Nat. Photon.* **1**, 293 (2007).
- [31] Tanabe, T., Kuramochi, E., Taniyama, H., and Notomi, M., “Electro-optic adiabatic wavelength shifting and  $q$  switching demonstrated using a p-i-n integrated photonic crystal nanocavity,” *Opt. Lett.* **35**, 3895–3897 (2010).
- [32] Yoshiki, W., Honda, Y., Kobayashi, M., Tetsumoto, T., and Tanabe, T., “Kerr-induced controllable adiabatic frequency conversion in an ultrahigh  $q$  silica toroid microcavity,” *Opt. Lett.* **41**, 5482–5485 (2010).
- [33] Minet, Y., Reis, L., Szabados, J., Werner, C. S., Zappe, H., Buse, K., and Breunig, I., “Pockels-effect-based adiabatic frequency conversion in ultrahigh- $q$  microresonators,” *arXiv*, 1909.07958 (2019).
- [34] Luennemann, M., Hartwig, U., Panotopoulos, G., and Buse, K., “Electrooptic properties of lithium niobate crystals for extremely high external electric fields,” *Appl. Phys. B* **76**, 403–406 (2003).